ENHANCEMENT OF GAS-FILLED MICROBUBBLE MAGNETIC SUSCEPTIBILITY BY IRON OXIDE NANOPARTICLES

A. M. Chow[1,2], J. S. Cheung[1,2], and E. X. Wu[1,2]

[1]Laboratory of Biomedical Imaging and Signal Processing, The University of Hong Kong, Hong Kong SAR, China, People's Republic of, [2]Department of Electrical and Electronic Engineering, The University of Hong Kong, Hong Kong SAR, China, People's Republic of

INTRODUCTION

Gas-filled microbubbles were originally developed as an intravascular contrast agent to enhance backscattering in ultrasound imaging. Microbubbles possess the ability to be an MR susceptibility contrast agent due to the induction of large local magnetic susceptibility differences by the gas-liquid interface. Feasibility of microbubbles as an MR pressure sensor, based on the susceptibility change caused by pressure-induced microbubble size change, has been explored through theoretical[1] and phantom[2] studies. Gas-filled microbubbles have also been shown as an MR susceptibility contrast agent *in vivo*[3]. However, microbubble susceptibility effect is relatively weak when compared with other intravascular MR susceptibility contrast agents. By optimizing the microbubble size distribution and choice of shell coating material and core gas, it is possible to substantially enhance the microbubble susceptibility effects[1] and reduce the dosage requirement for MR applications. In this study, we aim to demonstrate that microbubble susceptibility effects can be improved by embedding and entrapping iron oxide nanoparticles.

METHODS

Synthesis of iron oxide nanoparticles embedded albumin-coated microbubbles: Iron oxide nanoparticles embedded albumin-coated microbubbles (AMB) were produced by an adapted sonication method[4]. Briefly, 18 mg of monocrystalline iron oxide nanoparticles (MION; MGH) was added into a 5% solution of bovine serum albumin (10857, USB Corporation). The mixture was preheated to about 70°C and sonicated under aseptic conditions using an ultrasound frequency of 20 kHz. ***Synthesis of iron oxide nanoparticles entrapped polymeric microbubbles:*** Iron oxide nanoparticles entrapped polymeric microbubbles (polymeric MB) were produced by an adapted double emulsion method[5]. Briefly, 0.5g poly(D,L-lactide-*co*-glycolic acid 50:50, PLGA; Sigma) was dissolved in 10 mL of ethyl acetate (Sigma). 1 mL of MION solution (1.164mg/mL) was added to the polymer solution and probe sonicated for 30 s. The W/O emulsion was then poured into a 5% poly(vinyl alcohol) (PVA; Sigma) solution and homogenized for 5 min. The double (W/O)/W emulsion was then poured into a 2% isopropyl alcohol (Sigma) and stirred at room temperature for 1 hour. The capsules were collected by centrifugation, washed once with deionized water, centrifuged at 15°C for 5 min. at 3000*g* and the supernatant discarded. The capsules were then washed three times with hexane (Sigma). The capsules were frozen in a -80°C freezer and lyophilized using a freeze dryer to fully dry the capsules and sublime the encapsulated water. ***MRI and Data Analysis***: All MRI experiments were performed on a 7 T Bruker MRI scanner. Microbubble phantom study was performed with 38-mm quadrature resonator for RF transmission and receiving. AMB were diluted from a well-mixed microbubble suspension to 4% volume fraction with the addition of saline, while polymeric MB were prepared by adding saline of 2 mL to 50 mg of the lyophilized powder. The microbubbles were then placed in separate 2-mL cylindrical phantom tubes. Each phantom tube was slowly warmed to room temperature and gently mixed for 2 min outside the magnet prior to MR measurements. To ensure uniform suspension of microbubbles, the phantom was then continuously stirred by rotation inside the magnet. It was then arrested in horizontal position immediately before the start of MR acquisition sequence. Apparent transverse relaxation rate enhancement (ΔR_2^*) was measured by acquiring multi-echo gradient-echo (GE) signals continuously without phase encoding for 2 min from an axial 1-mm slice at middle of the phantom. The measurement was repeated six times for each microbubble phantom. The parameters were TR = 1000 ms, TE = 3.5, 7, 10.5, 14, 17.5, 21, 24.5, 28 ms, flip angle = 30º and NEX = 1. Phantom R_2^* values were computed by monoexponential fitting of the peak magnitudes of the multi-echo GE signals using a software toolkit developed in MATLAB (MathWorks). Initially, there was a uniform suspension of microbubbles. As GE signals were acquired, microbubbles started to migrate upward; therefore, in the final state the microbubbles aggregated in the upper part of the tube. Microbubble induced ΔR_2^* was then calculated as the difference between R_2^* in the initial state and that in the final state. To demonstrate that MION were embedded and entrapped, R_2^* was measured before and after cavitation, which was performed by applying ultrasound of frequency 40 kHz. R_2^* maps of the suspending solutions were acquired before and after cavitation with multiple gradient echo sequences. ***In vivo Demonstration***: Normal SD rats (~200-250 g) were injected intravenously with 0.2 mL of microbubble suspension (~4% volume fraction; N = 1 for AMB with MION and N = 1 for polymeric MB with MION) at a rate of 1.2 mL/min to avoid possible microbubble destruction due to high pressure and shear stress under femoral vein catheterization. Dynamic susceptibility weighted liver MRI was performed with respiratory-gated single-shot GE-EPI sequence under inhaled isoflurane anaesthesia using TR ≈ 1000 ms, TE = 10 ms, FA = 90º, FOV = 50 mm × 50 mm, slice thickness = 2 mm, acquisition matrix = 64 × 64, and NEX = 1.

RESULTS AND DISCUSSIONS

Values of R_2^* were plotted against time in Figure 1 for different microbubbles. As GE signals were acquired, microbubbles started to migrate upward; therefore, in the final state values of R_2^* were due to the suspending solution. The different amounts of free MION in the suspended solution accounted for the difference in the R_2^* of the suspending solution. Microbubble induced ΔR_2^* of different microbubbles were depicted in Figure 2. The MION embedded and entrapped would enhance the susceptibility effect and increased the values of ΔR_2^* as MION would float along with the microbubbles, resulting a larger ΔR_2^* values. Suspending solution R_2^* for AMB without and with MION after cavitation were found to be increased by 1.41 s^{-1} and 23.91 s^{-1} respectively. Similarly, suspending solution R_2^* for polymeric MB without and with MION after cavitation were found to be increased by 1.52 s^{-1} and 75.84 s^{-1} respectively. These substantial differences for microbubbles with MION demonstrate that there were more MION in the suspending solution after cavitation; suggesting that embedded and entrapped MION were released into suspending solution after the microbubble cavitation. Transmission electron microscopy was done on AMB with MION and depicted in Figure 3. MION as dark dots (red arrows) were observed on the shells of AMB, validating MION was embedded onto shells of AMB. Nevertheless, small amount of free MION was also observed in suspending solution (green arrow). Figure 4(a) shows one of the preinjection GE-EPI T_2^*-weighted images, while (b) shows the postinjection GE-EPI T_2^*-weighted image with the maximum susceptibility contrast for polymeric MB with MION injection. Figure 5 depicts the T_2^*-weighted signal time course during polymer MB with MION injection with ROI selected from homogeneous liver region (indicated in Figure 4(a)). Similar signal time course was also observed during AMB with MION injection. The T_2^*-weighted signals after microbubble injection did not return to the preinjection baseline, this may be caused by accumulation of released MION in Kupffer cells after *in vivo* microbubble clearance.

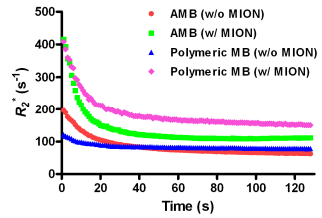

Figure 1 Values of R_2^* were plotted against time for different microbubbles.

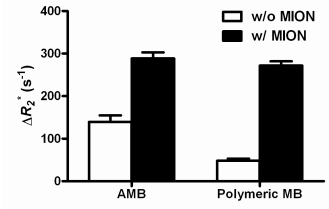

Figure 2 Microbubble induced ΔR_2^* of different microbubbles. The error bars represent one standard deviation.

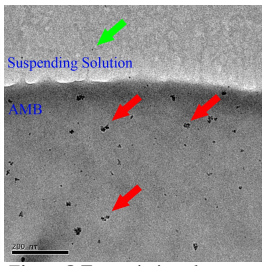

Figure 3 Transmission electron microsgraph shows MION was embedded onto shells of AMB.

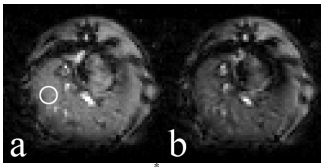

Figure 4 GE-EPI T_2^*-weighted image for polymeric MB w/ MION (a) preinjection image and (b) postinjection with the maximum susceptibility contrast.

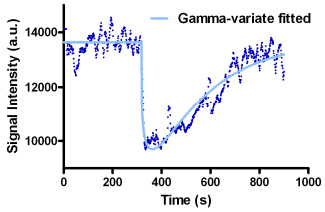

Figure 5 T_2^*-weighted signal time course in a homogenous liver region during polymeric MB w/ MION injection.

CONCLUSIONS

In this study, we demonstrated, for the first time, that embedding iron oxide nanoparticles onto shells of albumin-coated microbubbles and entrapping iron oxide nanoparticles in polymeric microbubbles is feasible. Work is currently underway to characterize the *in vivo* susceptibility effects of these microbubbles. With such approach, microbubble susceptibility can be significantly enhanced, so that microbubbles can be monitored with high sensitivity and low concentrations under MRI.

ACKNOWLEDGEMENTS

This work was supported by GRF7642/06M.

REFERENCES

[1] Dharmakumar R, et al., Magn Reson Med 2002;47(2):264-273. [2] Alexander AL, et al., Magn Reson Med 1996;35(6):801-806. [3] Wong KK, et al., Magn Reson Med 2004;52(3):445-452. [4] Cerny D, et al.; United States Patent 4957656. 1990. [5] El-Sherif DM, et al., J Biomed Mater Res A 2003;66(2):347-355.